HHS Public Access

Author manuscript

J Alzheimers Dis. Author manuscript; available in PMC 2018 June 12.

Published in final edited form as:

J Alzheimers Dis. 2016 ; 49(2): 329–342. doi:10.3233/JAD-150306.

White Matter Changes are Associated with Ventricular Expansion in Aging, Mild Cognitive Impairment, and Alzheimer's Disease

Jean-Philippe Coutu[a,b,*], **Alison Goldblatt**[a,c], **H. Diana Rosas**[a,d], **David H. Salat**[a,c,e], and **the Alzheimer's Disease Neuroimaging Initiative (ADNI)**[1]

[a]MGH/MIT/HMS Athinoula A. Martinos Center for Biomedical Imaging, Massachusetts General Hospital, Harvard Medical School, Charlestown, MA, USA

[b]Harvard-MIT Division of Health Sciences and Technology, Massachusetts Institute of Technology, Cambridge, MA, USA

[c]Department of Radiology, Massachusetts General Hospital, Harvard Medical School, Boston, MA, USA

[d]Department of Neurology, Massachusetts General Hospital, Harvard Medical School, Boston, MA, USA

[e]Neuroimaging Research for Veterans Center, VA Boston Healthcare System, Boston, MA, USA

Abstract

White matter lesions are highly prevalent in individuals with Alzheimer's disease (AD). Although these lesions are presumed to be of vascular origin and linked to small vessel disease in older adults, little information exists about their relationship to markers of classical AD neurodegeneration. Thus, we examined the link between these white matter changes (WMC) segmented on T_1-weighted MRI and imaging markers presumed to be altered due to primary AD neurodegenerative processes. Tissue microstructure of WMC was quantified using diffusion tensor imaging and the relationship of WMC properties and volume to neuroimaging markers was examined in 219 cognitively healthy older adults and individuals with mild cognitive impairment and AD using data from the Alzheimer's Disease Neuroimaging Initiative. No significant group differences in WMC properties were found. However, there were strong associations between diffusivity of WMC and ventricular volume, volume of WMC and total WM volume. In comparison, group differences in parahippocampal white matter microstructure were found for all diffusion metrics and were largely explained by hippocampal volume. Factor analysis on

[*]Correspondence to: Jean-Philippe Coutu, Division of Health Sciences and Technology, Massachusetts Institute of Technology, Building E25-518, 77 Massachusetts Avenue, Cambridge, 02139-4307 MA, USA. Tel.: +1 857 318 9617; Fax: +1 617 253 6692; coutu@nmr.mgh.harvard.edu.

[1]Data used in preparation of this article were obtained from the Alzheimer's Disease Neuroimaging Initiative (ADNI) database (http://adni.loni.usc.edu). As such, the investigators within the ADNI contributed to the design and implementation of ADNI and/or provided data but did not participate in analysis or writing of this report. A complete listing of ADNI investigators can be found at http://adni.loni.usc.edu/wp-content/uploads/how_to_apply/ADNI_Acknowledgement_List.pdf.

Authors' disclosures available online (http://j-alz.com/manuscript-disclosures/15-0306r3).

SUPPLEMENTARY MATERIAL

The supplementary material is available in the electronic version of this article: http://dx.doi.org/10.3233/JAD-150306.

neuroimaging markers suggested two independent sets of covarying degenerative changes, with potentially age- and vascular-mediated tissue damage contributing to one factor and classical neurodegenerative changes associated with AD contributing to a second factor. These data demonstrate two potentially distinct classes of degenerative change in AD, with one factor strongly linked to aging, ventricular expansion, and both volume and tissue properties of white matter lesions, while the other factor related to classical patterns of cortical and hippocampal neurodegeneration in AD.

Keywords

Alzheimer's disease; cerebral ventricles; diffusion tensor imaging; hippocampus; leukoaraiosis; mild cognitive impairment; white matter

INTRODUCTION

Magnetic resonance imaging (MRI) measures of hippocampal volume and cortical thickness have been shown to predict incident Alzheimer's disease (AD) [1–5] and to correlate with classical histopathological measures of AD [6, 7]. Less widely recognized is that total volume of white matter (WM) lesions also increases with [8–10] and is predictive of [11–14] mild cognitive impairment (MCI) and AD, though not in every study [5, 15]. These lesions, also called leukoaraiosis, are typically identified *in vivo* as WM signal hyperintensities of presumed vascular origin on neuroimaging [16] due to their appearance on T_2-weighted and fluid-attenuated inversion recovery (FLAIR) MRI. They can also be observed as moderately hypointense regions in WM on T_1-weighted MRI (however not well distinguished from infarcted tissue). Epidemiological studies demonstrate that these WM lesions are associated with small vessel disease [17, 18], hypertension [9, 19–23], and other vascular risk factors [9, 22–24, 24] in non-demented individuals. MRI and SPECT studies confirm their lower perfusion compared to normal-appearing WM [27–31]. While lesion volume is known to be increased in AD [8–10, 13, 32], limited evidence exists to demonstrate that the WM lesions present in AD are similar in nature to those observed in non-demented older individuals [9, 33, 34]. Relatively few pathological studies have been conducted, most of them showing increased demyelination and axonal loss, and more severe gliosis and denudation of the ventricular ependyma in the lesions of AD compared to the lesions of non-demented controls [8, 35, 36]. Additionally, little is known about how this typically vascular-associated tissue damage relates to more classical imaging markers of AD pathology [37–39], such as cortical thickness and hippocampal volume, which could provide important information about how this tissue damage fits with the classical and diagnostic pathophysiologic properties of the disease.

We segmented WM lesions automatically with the FreeSurfer analysis stream using T_1-weighted images. While this segmentation was chosen for its automation and convenience, we note that this procedure does not differentiate white matter changes (WMC) typically measured as 'hyperintensities' from lacunar infarcts, though infarcts are much less prevalent and contribute a much smaller volume [19, 20]. We refer to the WM segmentation studied here as WMC, which may be measuring similar underlying pathology as those from

standard T_2-weighted and FLAIR methods based on highly correlated volumetric results as detailed in the methods. We examined volume and tissue properties of WMC in a sample of controls, MCI, and AD to better understand how these markers relate to common degenerative processes in AD. Results were compared to other types of WM damage including changes in the normal-appearing white matter (NAWM) globally and in the parahippocampal WM which exhibited microstructural changes in prior work in AD [38]. The parahippocampal WM was considered a 'pathology control' to determine whether the effects within the lesions were truly unique and distinct from a more classical AD effect potentially secondary to cortical degeneration.

MATERIALS AND METHODS

Participants and MRI acquisition

A large publicly-available dataset from the Alzheimer's Disease Neuroimaging Initiative (ADNI, http://adni.loni.usc.edu) included 74 controls, 97 participants with MCI, and 48 participants with AD who underwent whole-brain MRI scanning at one or multiple visits on a 3-Tesla GE Medical Systems scanner and had sagittal T_1-weighted 3D spoiled gradient echo images and diffusion-weighted images (b = 1000 s/mm^2, 41 directions) available at the time of download. These datasets were acquired using previously described ADNI Core MRI and DTI protocols [41]. Four participants (one control, one with MCI, and two with AD) were excluded because of extensive WM damage or ventricular enlargement which led to unreliable automated results using the methods described below. Group designation of control, MCI, and probable AD was determined by ADNI based on the criteria of the National Institute of Neurological and Communicative Diseases and Stroke-Alzheimer's Disease and Related Disorders Association [42]. Participants enrolled as normal or with significant memory concern and with a Clinical Dementia Rating [43] of 0 were grouped together into the control group, and participants enrolled as early and late MCI were combined into one MCI group (see ADNI 2 Procedures Manual on http://www.adni-info.org for more information). Clinical profiles and diagnostic information were obtained from the assessment closest in time to the MRI acquisition. A subgroup of individuals with a volume of WMC greater than 1% of total WM volume was also examined to assure that results were not skewed by individuals with small volumes of WMC. Demographics both for this subgroup and for the entire group are provided in Table 1. Written informed consent was obtained from all participants or their representatives through ADNI. The study procedures were approved by institutional review boards of all participating institutions.

Diffusion data processing

The diffusion dataset was corrected for 3D head motion and eddy current distortion using FSL (http://www.fmrib.ox.ac.uk/fsl), and translation and rotation motion estimates were obtained from the registration matrices [44]. For individuals with multiple available datasets, we picked the one with the least average translation motion. The diffusion tensor imaging (DTI) model was fit to the diffusion dataset and mean, axial, and radial diffusivity (MD, DA, and DR, respectively) as well as fractional anisotropy (FA) were obtained using FSL.

Automated subcortical and WMC segmentation

Automated subcortical and WM segmentation as well as cortical surface reconstruction were obtained from the T_1-weighted images using FreeSurfer (http://surfer.nmr.mgh.harvard.edu) [45, 46]. Segmentations of the entorhinal and parahippocampal WM were combined into a single segmentation that we referred to here as parahippocampal WM. The automated segmentation also included a WMC segmentation that is conservative relative to T_2-weighted and FLAIR MRI and segmented only the most obvious WMC identifiable on T_1-weighted images. FreeSurfer mri_relabel_hypointensities was used to refine the WMC segmentation using the surface reconstruction. We found a correlation coefficient of 0.96 (n = 112) between the volume of WMC obtained with FreeSurfer and the WM hyperintensity volume obtained with FLAIR MRI and tissue priors using publicly-available values from ADNI. However, the WM hyperintensity volume obtained with FLAIR MRI was on average 1.14 times greater than the volume obtained with FreeSurfer, which was more conservative. Examples of T_1-weighted hypointensities and their WMC segmentation in controls and individuals with MCI and AD are provided in Supplementary Figure 1. Total WM volume, parahippocampal WM volume, ventricular volume (lateral ventricles), and hippocampal volume were normalized as a volume percentage of estimated total intracranial volume in each individual. The natural logarithm of the volume of WMC divided by total WM volume was used for all statistical analyses to obtain a more normalized distribution of this typically skewed measure. Additionally, FreeSurfer was used to extract measures of cortical thickness from cortical surface labels representing the regions that undergo thinning in early AD, previously described as the cortical signature of AD given the reliability of this effect across samples [1, 2, 47]. The average cortical thickness weighted by the surface area of each label has been used as a specific measure of cortical atrophy in AD and will be referred to here as the AD signature cortical thickness or simply as cortical thickness. This cortical signature did not include the hippocampus as this structure has unique anatomy compared to the regions of the cortical mantle modeled here as a two-dimensional sheet for the measurement of cortical thickness. Additionally, the hippocampus is a unique structure known to be vulnerable to both AD and vascular pathology [48, 49] and therefore may have unique properties compared to cortical structures included in the AD signature calculation (which includes neocortex as well as other types of cortex).

Registration procedures and normative data calculation

The diffusion-weighted images were registered to the anatomical series using FreeSurfer boundary-based registration [50]. Average DTI metrics within the WMC segmentations were obtained for each individual in diffusion native space. A segmentation of the NAWM was created from the subtraction of the WMC segmentation from the total WM segmentation in native diffusion space. Furthermore, a WM skeleton mask was created using FSL Tract-Based Spatial Statistics [51] and was used to reduce partial volume effects when calculating average DTI values coming from both NAWM and parahippocampal WM in native diffusion space, as described in previous work [52]. Each individual's anatomical series was registered to the MNI152 common space using FSL FLIRT and FNIRT to allow comparison of the anatomical segmentations and extract group maps of the WMC prevalence in each voxel. Diffusion maps were warped to this common space using FSL to create normative diffusion maps by averaging maps from all subjects with a volume of WMC less than 1% of total WM

volume. These normative averages were then warped back to the native diffusion space of every subject. This procedure was performed to determine the difference between diffusion metrics inside WMC and normative diffusion metrics in the same regions for each individual, and therefore account for the varying inter-individual location of WMC in our analyses.

Statistical analyses

Statistical analyses were performed using JMP 10 statistical software (SAS Institute Inc., Cary, NC, USA). Post-hoc Tukey HSD tests were performed to assess for any significant differences between groups for the volume and DTI metrics of each structure, using age, gender, education [53], and motion measures (average translation and average rotation [44]) as covariates. Individuals with a volume of WMC less than 1% of total WM volume were excluded from statistical analyses of DTI metrics in WMC since they generally had few WMC voxels which were close to the ventricles and for which ROI averages of diffusion metrics were more similar to the ventricles, likely due to partial-volume effects. Strong correlations were observed between the AD signature cortical thickness, hippocampal, ventricular and total WM volumes and the volume of WMC (all significant pairwise, see Supplementary Figure 2). Therefore, general linear models including group, age, gender, education, motion measures, and these five measures were used to understand which individual measures explained the variance in diffusion metrics independently of all other variables. In addition, to account for the fact that variance in diffusion metrics might be explained by a phenomenon that is not unique to any individual measure, factor analysis (with VARIMAX) was performed to obtain the primary factors representing the different sources of covariation within these five measures. These significant factors were then used with the same covariates in general linear models to understand their associations with the diffusion metrics. Group by marker/factor interactions were not included as they were not significant when added to the models. All results were corrected for multiple comparisons with Bonferroni (3 WM regions/comparisons for group differences in volume and 3 WM regions × 4 diffusion metrics = 12 primary comparisons for all results involving DTI) and estimated parameters were provided in the models in addition to *p*-values to ease interpretation. The same models including the number of APOE $\varepsilon 4$ alleles as an additional variable are presented as Supplementary Tables 1 and 2 in individuals with this information.

Alzheimer's Disease Neuroimaging Initiative

Data used in the preparation of this article were obtained from the Alzheimer's Disease Neuroimaging Initiative (ADNI) database (http://adni.loni.usc.edu). The ADNI was launched in 2003 by the National Institute on Aging (NIA), the National Institute of Biomedical Imaging and Bioengineering (NIBIB), the Food and Drug Administration (FDA), private pharmaceutical companies and non-profit organizations, as a $60 million, 5-year public-private partnership. The primary goal of ADNI has been to test whether serial MRI, positron emission tomography (PET), other biological markers, and clinical and neuropsychological assessment can be combined to measure the progression of MCI and early AD. Determination of sensitive and specific markers of very early AD progression is intended to aid researchers and clinicians to develop new treatments and monitor their effectiveness, as well as lessen the time and cost of clinical trials.

The Principal Investigator of this initiative is Michael W. Weiner, MD, VA Medical Center and University of California – San Francisco. ADNI is the result of efforts of many coinvestigators from a broad range of academic institutions and private corporations, and subjects have been recruited from over 50 sites across the U.S. and Canada. The initial goal of ADNI was to recruit 800 subjects but ADNI has been followed by ADNI-GO and ADNI-2. To date these three protocols have recruited over 1500 adults, ages 55 to 90, to participate in the research, consisting of cognitively normal older individuals, people with early or late MCI, and people with early AD. The follow up duration of each group is specified in the protocols for ADNI-1, ADNI-2 and ADNI-GO. Subjects originally recruited for ADNI-1 and ADNI-GO had the option to be followed in ADNI-2. For up-to-date information, see http://www.adni-info.org.

RESULTS

Group differences in prevalence and tissue properties of WMC

Qualitative examination suggested that the spatial distribution of WMC was similar across groups as previously described [10] (Fig. 1A). The subtractions between groups shown in Fig. 1B suggested greater prevalence of WMC in posterior areas for MCI compared to controls and greater prevalence of WMC in anterior areas for AD compared to MCI. However, voxel-wise differences in prevalence were only significant between AD and controls (corrected $p < 0.05$ using FSL randomize with threshold-free cluster enhancement, not shown).

Group differences in volume of WMC were significant between AD and controls (corrected $p < 0.01$) as shown in Fig. 2A. No significant group differences were observed for diffusion metrics within WMC. Normalization of diffusion measures to account for the differential location of the lesions across individuals reduced the standard error of group averages but group differences were still not significant. This is contrasted by several significant group differences in volume and diffusion properties for the parahippocampal WM as shown in Fig. 2B and a few significant group differences in total WM volume and NAWM diffusion properties as shown in Fig. 2C.

Associations between tissue properties of WMC and neuroimaging markers of AD

In Model 1, we tested whether diffusion metrics of WMC were associated with neuroimaging markers to determine if they would be uniquely related to hippocampal volume and cortical thickness. We found significant associations between increased diffusivity of WMC and increased ventricular volume (MD, DA, DR: corrected $p < 0.001$), decreased volume of WMC (MD, DR: corrected $p < 0.05$; DA: corrected $p < 0.01$) and decreased total WM volume (DR: corrected $p < 0.05$), independently of each other (see Table 2 for details). No associations were significant between diffusion metrics of WMC and hippocampal volume or cortical thickness, with the exception of increased FA of WMC being associated with decreased cortical thickness (corrected $p < 0.05$).

In Model 2, we tested in comparison whether parahippocampal WM diffusion metrics were associated with neuroimaging markers to determine if they would be primarily related to

hippocampal volume and cortical thickness. Increased diffusivity of parahippocampal WM was associated with hippocampal volume (MD, DR: corrected $p < 0.01$; DA: corrected $p < 0.05$) (see Table 2 for details). We additionally found an association between total WM volume and FA of the parahippocampal WM (corrected $p < 0.05$).

In Model 3, we tested whether NAWM diffusion metrics were associated with neuroimaging markers to confirm if they would be most associated with the volume of WMC as shown in prior work examining cognitively healthy older adults [54], but also possibly minimally associated with hippocampal volume and cortical thickness. As expected, we found significant associations between greater volume of WMC and both greater NAWM diffusivity and lower NAWM FA (MD, DR, FA: corrected $p < 0.001$). However, we also found additional, independent associations between lower total WM volume and both greater DR (corrected $p < 0.05$) and lower FA (corrected $p < 0.01$) and no associations involving either hippocampal volume or cortical thickness (see Table 2 for details).

Of note, group determination was not found to be significant in any model. There were no significant group by imaging marker interactions when they were included in any of the models.

Classes of degenerative change and associations with tissue properties of WMC

Factor analysis yielded two significant factors (Table 3). Both factors showed a high loading from hippocampal volume. Factor 1 otherwise included high loadings (>0.4) from volume of WMC, total WM volume, and ventricular volume, reflecting processes that are demonstrated in prior work to change with age and vascular disease in particular for volume of WMC [9, 19–26]. Factor 2 included the AD signature cortical thickness in addition to the hippocampal volume and therefore represented processes that are often used as imaging estimates of neurodegenerative changes in AD. Both factors were altered in individuals with AD compared to controls. Factor 1 had a stronger age effect and a weaker MMSE effect than Factor 2. See Fig. 3 for details.

In Model 4, we tested whether diffusion metrics of WMC were associated with any or both factors to determine if they would be related to the ‘age- and vascular-associated’ factor (Factor 1) and unrelated to the ‘neurodegenerative’ factor (Factor 2). We found strong significant associations between diffusivity of WMC and Factor 1 (MD, DA, DR: corrected $p < 0.001$) while DA and FA of WMC showed an association with Factor 2 (DA: corrected $p < 0.01$; FA: corrected $p < 0.001$) (see Table 4 for details).

In Model 5, we tested in comparison whether parahippocampal WM diffusion metrics were associated with any or both factors to determine if they would be mainly related to the ‘neurodegenerative’ factor (Factor 2). However, significant associations were found between parahippocampal WM diffusion metrics and both Factor 1 (MD, DR, FA: corrected $p < 0.001$) and Factor 2 (DR, FA: corrected $p < 0.01$; MD: corrected $p < 0.05$), independently of each other (see Table 4 for details).

In Model 6, we tested whether NAWM diffusion metrics were associated with any or both factors to determine if they would be mainly related to the ‘age- and vascular-associated’

factor (Factor 1) and minimally associated with the 'neurodegenerative' factor (Factor 2). We found significant associations between all diffusion measures in NAWM and Factor 1 (MD, DR, and FA: corrected $p < 0.001$; DA: corrected $p < 0.01$) and weaker associations between NAWM diffusivity and Factor 2 (MD, DR: corrected $p < 0.05$). Factor 2 had an effect size on diffusivity values averaging less than half the effect size of Factor 1 (see Table 4 for details).

Of note, group determination was not found to be significant in any model. There were no significant group by imaging marker interactions when they were included in any of the models.

DISCUSSION

We observed in this study that individuals with AD had greater volumes of WMC than non-demented older adults as demonstrated in prior work; however, the diffusion values within WMC did not differ across groups. Parahippocampal WM, which may be more likely to undergo changes secondary to medial temporal cortex neurodegeneration as part of classical AD, showed consistent group differences for all diffusion metrics, which were most correlated with hippocampal volume. Diffusion measures of WMC correlated instead significantly with ventricular, WMC, and total WM volumes independently. Furthermore, we demonstrated two independent classes of degenerative changes in AD through factor analysis of hippocampal volume, AD signature cortical thickness, ventricular volume, total WM volume, and volume of WMC. One factor was more strongly associated with age and diffusivity and total volume of WMC, which are typically presumed to be of vascular origin; yet the factor was strongly affected in individuals with AD compared to controls. The second factor was more strongly related to MMSE and imaging markers of AD neurodegeneration, such as cortical thickness, and was associated with worse parahippocampal WM microstructure. Critically, a significant amount of variance in two commonly examined markers of change in AD, ventricular volume and hippocampal volume, factored with the volume of WMC and therefore demonstrated a potential degenerative link between vascular conditions and changes commonly attributed to classical AD neurodegenerative processes. As hippocampal volume was retained as an important marker in both factors, we further investigated its major determinants. Greater age, reduced AD signature cortical thickness, reduced total WM volume, and greater ventricular and WMC volumes were all associated with a lower hippocampal volume and each accounted for significant, independent additional variance explained, even when taking into account group determination in the model. These associations, especially with age, WMC, and total WM volumes, might be key to understanding the presumed vascular component of AD pathogenesis and its influence on the hippocampus [48, 49] and require further investigation.

The current results demonstrate the need for better understanding of the increase in ventricular and WMC volumes observed in MCI and AD. Indeed, ventricular enlargement better explained the diffusion measures in WMC than any other variable including volume of WMC and total WM volume, and was mainly related to an increase in average diffusivity. Diffusivity of WMC also seemed to be increased with decreased volume of WMC; however, this effect was apparent only as an independent effect from ventricular volume and total WM

volume, which were also included in the general linear model. Without those covariates, greater volume of WMC indeed related to greater diffusivity within WMC (not shown). Furthermore, once the underlying process shared by these imaging markers was commonly represented by the 'age- and vascular-associated' factor, greater volume of WMC, as part of that factor, related to greater diffusivity of WMC. It is still interesting to note that some residual variance of WMC diffusivity was accounted for by WMC volume as an independent effect from this common factor, suggesting possibly two types of WMC such as mild and diffuse WMC and more severe, localized WMC. Similarly, both total WM and ventricular volumes also had independent associations with diffusivity of WMC. Interestingly, group differences in diffusion metrics of WMC could have been expected given the group differences in ventricular volume and volume of WMC and their associations with diffusion metrics of WMC. However, this is likely due to some degree to the residual variance not explained by the correlation between diffusion metrics of WMC and both ventricular and WMC volume and to group differences in diffusion metrics of WMC being simply slightly under significance threshold. Diffusion metrics of WMC also tracked better with ventricular volume, volume of WMC, and total WM volume than with group differentiation, despite the fact those imaging markers were affected with disease. It is also interesting to note that the associations between imaging markers and diffusion metrics did not differ significantly between groups. Finally, while there was an association between FA of WMC and regional cortical thickness, it was in the opposite direction than would be expected in the case of a neurodegenerative effect (increased FA was associated with reduced cortical thickness). While this effect should be further investigated, it remains that there was a much stronger effect size of the 'age- and vascular-associated' factor than the 'neurodegenerative' factor on the diffusivity of WMC (nearly by a factor of three). Similarly, the effect size of the 'age- and vascular-associated' factor was greater than the effect size of the 'neurodegenerative' factor on diffusion measures of both parahippocampal WM and NAWM, though to a lesser degree than on diffusion measures of WMC. These results hint at a dissociation between the presumed neurodegenerative effects of AD and the microstructural changes of WM and especially of the more prevalent WMC observed in AD.

One phenomenon we speculate may explain the strong relationship found in this study between increasing ventricular volume and diffusivity of WMC, independently of decreasing total WM volume, is the denudation of the ventricular ependyma, which is severe in AD [8] and may permit leakage of cerebrospinal fluid into the WM tissue as suggested in prior work [8, 55]. Other potential causes of water dysregulation have been recently investigated in the context of AD and could explain the association between the diffusivity in WMC and ventricular volume [56]. In particular, increased or dysregulated aquaporin expression of the subependymal cells and other cells lining the lateral ventricles [57] as well as blood-brain barrier disruption [58, 59] may also lead concurrently to ventricular expansion and the formation of edema in WMC [60]. It is possible that overall dysfunction of the ventricular lining might be a precipitating factor or provide a 'second hit' to more classical AD neurodegenerative processes in the development of clinically diagnosed AD. However, clinical manifestation of AD in the relative absence of WMC has been reportedly observed and therefore such lesions may not be a necessary component of the disorder.

To our knowledge, this is the first report that takes into account the diffusion properties of the normative anatomy. Specifically, diffusion values within WMC were strongly dependent on the normative values which varied with the underlying anatomy (e.g., in regions with single straight fibers versus crossing fibers), underlying the importance of considering these values when calculating the degree of tissue damage within WMC.

The current work is limited in that the findings are cross-sectional and do not provide information about the mechanisms of the associations reported. Follow-up longitudinal and interventional work would be valuable to determine whether these associations continue to track with time and whether a therapeutic reduction in one type of change is followed by a reduction in one or more of the associated markers. Another limitation is the possible inclusion of lacunar infarcts in the segmentation of WMC as those are also hypointense on T_1-weighted imaging. However, they have lower prevalence and much lower volume than more common WMC identified as WM hyperintensity on T_2-weighted and FLAIR imaging. While lacunar infarcts may be responsible for the relationship between decreasing volume of WMC and increasing diffusivity of WMC, this association was independent of the key association between greater ventricular volume and greater diffusivity of WMC. Regardless of these limitations, the current work demonstrates that WMC are linked to other traditional imaging markers of AD and provide novel information about the complex inter-associational properties of several known markers of AD potentially providing information about multiple ‘classes’ of partially independent degenerative change to be targeted for therapeutic intervention.

Supplementary Material

Refer to Web version on PubMed Central for supplementary material.

Acknowledgments

We would like to thank Paul J. Wilkens for his help with the processing of the diffusion images. This study was supported by the NIH grant R01NR010827 and by Biogen Idec using resources provided by NIH grants NS042861, NS058793 and by the Center for Functional Neuroimaging Technologies, P41RR14075, a P41 Regional Resource supported by the Biomedical Technology Program of the National Center for Research Resources (NCRR), NIH. This work also involved the use of instrumentation supported by the NCRR Shared Instrumentation Grant Program and/or High-End Instrumentation Grant Program; specifically, grant numbers S10RR021110, S10RR023401, S10RR019307, S10RR019254 and S10RR023043. J.P.C. was supported by the Fonds Québécois de la Recherche – Santé and by the HST IDEA2 Program supported by the Peter C. Farrell (1967) Fund.

Data collection and sharing for this project was funded by the Alzheimer’s Disease Neuroimaging Initiative (ADNI) (NIH Grant U01 AG024904) and DOD ADNI (Department of Defense award number W81XWH-12-2-0012). ADNI is funded by the National Institute on Aging, the National Institute of Biomedical Imaging and Bioengineering, and through generous contributions from the following: Alzheimer’s Association; Alzheimer’s Drug Discovery Foundation; Araclon Biotech; BioClinica, Inc.; Biogen Idec Inc.; Bristol-Myers Squibb Company; Eisai Inc.; Elan Pharmaceuticals, Inc.; Eli Lilly and Company; EuroImmun; F. Hoffmann-La Roche Ltd and its affiliated company Genentech, Inc.; Fujirebio; GE Healthcare; IXICO Ltd.; Janssen Alzheimer Immunotherapy Research & Development, LLC.; Johnson & Johnson Pharmaceutical Research & Development LLC.; Medpace, Inc.; Merck & Co., Inc.; Meso Scale Diagnostics, LLC.; NeuroRx Research; Neurotrack Technologies; Novartis Pharmaceuticals Corporation; Pfizer Inc.; Piramal Imaging; Servier; Synarc Inc.; and Takeda Pharmaceutical Company. The Canadian Institutes of Health Research is providing funds to support ADNI clinical sites in Canada. Private sector contributions are facilitated by the Foundation for the National Institutes of Health (http://www.fnih.org). The grantee organization is the Northern California Institute for Research and Education, and the study is coordinated by the Alzheimer’s Disease Cooperative Study at the University of California, San Diego. ADNI data are disseminated by the Laboratory for Neuro Imaging at the University of Southern California.

References

1. Bakkour A, Morris JC, Dickerson BC. The cortical signature of prodromal AD: Regional thinning predicts mild AD dementia. Neurology. 2009; 72:1048–1055. [PubMed: 19109536]
2. Dickerson BC, Stoub TR, Shah RC, Sperling RA, Killiany RJ, Albert MS, Hyman BT, Blacker D, Detoledo-Morrell L. Alzheimer-signature MRI biomarker predicts AD dementia in cognitively normal adults. Neurology. 2011; 76:1395–1402. [PubMed: 21490323]
3. Jack CR Jr, Petersen RC, Xu YC, O'Brien PC, Smith GE, Ivnik RJ, Boeve BF, Waring SC, Tangalos EG, Kokmen E. Prediction of AD with MRI-based hippocampal volume in mild cognitive impairment. Neurology. 1999; 52:1397–1403. [PubMed: 10227624]
4. Whitwell JL, Shiung MM, Przybelski SA, Weigand SD, Knopman DS, Boeve BF, Petersen RC, Jack CR Jr. MRI patterns of atrophy associated with progression to AD in amnestic mild cognitive impairment. Neurology. 2008; 70:512–520. [PubMed: 17898323]
5. Kantarci K, Weigand SD, Przybelski SA, Shiung MM, Whitwell JL, Negash S, Knopman DS, Boeve BF, O'Brien PC, Petersen RC, Jack CR Jr. Risk of dementia in MCI: Combined effect of cerebrovascular disease, volumetric MRI and 1H MRS. Neurology. 2009; 72:1519–1525. [PubMed: 19398707]
6. Archer HA, Edison P, Brooks DJ, Barnes J, Frost C, Yeatman T, Fox NC, Rossor MN. Amyloid load and cerebral atrophy in Alzheimer's disease: An 11C-PIB positron emission tomography study. Ann Neurol. 2006; 60:145–147. [PubMed: 16802294]
7. Jack CR Jr, Dickson DW, Parisi JE, Xu YC, Cha RH, O'Brien PC, Edland SD, Smith GE, Boeve BF, Tangalos EG, Kokmen E, Petersen RC. Antemortem MRI findings correlate with hippocampal neuropathology in typical aging and dementia. Neurology. 2002; 58:750–757. [PubMed: 11889239]
8. Scheltens P, Barkhof F, Leys D, Wolters EC. Histopathologic correlates of white matter changes on MRI in Alzheimer's disease and normal aging. Neurology. 1995; 45:883–888. [PubMed: 7746401]
9. Yoshita M, Fletcher E, Harvey D, Ortega M, Martinez O, Mungas DM, Reed BR, DeCarli CS. Extent and distribution of white matter hyperintensities in normal aging, MCI, and AD. Neurology. 2006; 67:2192–2198. [PubMed: 17190943]
10. Holland CM, Smith EE, Csapo I, Gurol ME, Brylka DA, Killiany RJ, Blacker D, Albert MS, Guttmann CRG, Greenberg SM. Spatial distribution of white-matter hyperintensities in Alzheimer disease, cerebral amyloid angiopathy, and healthy aging. Stroke. 2008; 39:1127–1133. [PubMed: 18292383]
11. Smith EE, Egorova S, Blacker D, Killiany RJ, Muzikansky A, Dickerson BC, Tanzi RE, Albert MS, Greenberg SM, Guttmann CRG. Magnetic resonance imaging white matter hyperintensities and brain volume in the prediction of mild cognitive impairment and dementia. Arch Neurol. 2008; 65:94–100. [PubMed: 18195145]
12. Provenzano FA, Muraskin J, Giuseppe T, Narkhede A, Wasserman BT, Griffith EY, Guzman VA, Meier IB, Zimmerman ME, Brickman AM. White matter hyperintensities and cerebral amyloidosis: Necessary and sufficient for clinical expression of Alzheimer disease? JAMA Neurol. 2013; 70:455–461. [PubMed: 23420027]
13. Brickman AM, Provenzano FA, Muraskin J, Manly JJ, Blum S, Apa Z, Stern Y, Brown T, Luchsinger J, Mayeux R. Regional white matter hyperintensity volume, not hippocampal atrophy, predicts incident Alzheimer disease in the community. Arch Neurol. 2012; 69:1621–1627. [PubMed: 22945686]
14. Mortamais M, Artero S, Ritchie K. White matter hyperintensities as early and independent predictors of Alzheimer's disease risk. J Alzheimers Dis. 2014; 42:S393–S400. [PubMed: 25261452]
15. DeCarli C, Mungas D, Harvey D, Reed B, Weiner M, Chui H, Jagust W. Memory impairment, but not cerebrovascular disease, predicts progression of MCI to dementia. Neurology. 2004; 63:220–227. [PubMed: 15277612]
16. Wardlaw JM, Smith EE, Biessels GJ, Cordonnier C, Fazekas F, Frayne R, Lindley RI, O'Brien JT, Barkhof F, Benavente OR, Black SE, Brayne C, Breteler M, Chabriat H, Decarli C, de Leeuw F-E, Doubal F, Duering M, Fox NC, Greenberg S, Hachinski V, Kilimann I, Mok V, Oostenbrugge R, Van Pantoni L, Speck O, Stephan BCM, Teipel S, Viswanathan A, Werring D, Chen C, Smith C,

van Buchem M, Norrving B, Gorelick PB, Dichgans M. Neuroimaging standards for research into small vessel disease and its contribution to ageing and neurodegeneration. Lancet Neurol. 2013; 12:822–838. [PubMed: 23867200]

17. Pantoni L. Cerebral small vessel disease: From pathogenesis and clinical characteristics to therapeutic challenges. Lancet Neurol. 2010; 9:689–701. [PubMed: 20610345]
18. Gouw AA, Seewann A, Flier WM, Van Der Barkhof F, Rozemuller AM, Scheltens P, Geurts JJG. Heterogeneity of small vessel disease: A systematic review of MRI and histopathology correlations. J Neurol Neurosurg Psychiatry. 2011; 82:126–135. [PubMed: 20935330]
19. Chen X, Wen W, Anstey KJ, Sachdev PS. Prevalence, incidence and risk factors of lacunar infarcts in a community sample. Neurology. 2009; 73:266–272. [PubMed: 19636046]
20. DeCarli C, Mungas D, Harvey D, Reed B, Weiner M, Chui H, Jagust W. Memory impairment, but not cerebrovascular disease, predicts progression of MCI to dementia. Neurology. 2004; 63:220–227. [PubMed: 15277612]
21. Rostrup E, Gouw AA, Vrenken H, van Straaten ECW, Ropele S, Pantoni L, Inzitari D, Barkhof F, Waldemar G. The spatial distribution of age-related white matter changes as a function of vascular risk factors–results from the LADIS study. Neuroimage. 2012; 60:1597–1607. [PubMed: 22305990]
22. Stenset V, Johnsen L, Kocot D, Negaard A, Skinningsrud A, Gulbrandsen P, Wallin A, Fladby T. Associations between white matter lesions, cerebrovascular risk factors, and low CSF Abeta42. Neurology. 2006; 67:830–833. [PubMed: 16966546]
23. Jeerakathil T, Wolf PA, Beiser A, Massaro J, Seshadri S, D'Agostino RB, DeCarli C. Stroke risk profile predicts white matter hyperintensity volume: The Framingham Study. Stroke. 2004; 35:1857–1861. [PubMed: 15218158]
24. Murray AD, Staff RT, Shenkin SD, Deary IJ. Brain white matter hyperintensities: Relative importance of vascular risk factors in nondemented elderly people. Radiology. 2005; 237:251–257. [PubMed: 16126931]
25. Gottesman RF, Coresh J, Catellier DJ, Sharrett AR, Rose KM, Coker LH, Shibata DK, Knopman DS, Jack CR Jr, Mosley TH. Blood pressure and white-matter disease progression in a biethnic cohort: Atherosclerosis risk in communities (ARIC) study. Stroke. 2010; 41:3–8. [PubMed: 19926835]
26. Breteler MM, van Swieten JC, Bots ML, Grobbee DE, Claus JJ, van den Hout JH, van Harskamp F, Tanghe HL, de Jong PT, van Gijn J. Cerebral white matter lesions, vascular risk factors, and cognitive function in a population-based study: The Rotterdam Study. Neurology. 1994; 44:1246–1252. [PubMed: 8035924]
27. Marstrand JR. Cerebral perfusion and cerebrovascular reactivity are reduced in white matter hyperintensities. Stroke. 2002; 33:972–976. [PubMed: 11935046]
28. Bastos-Leite AJ, Kuijer JPA, Rombouts SARB, Sanz-Arigita E, van Straaten EC, Gouw AA, van der Flier WM, Scheltens P, Barkhof F. Cerebral blood flow by using pulsed arterial spin-labeling in elderly subjects with white matter hyperintensities. Am J Neuroradiol. 2008; 29:1296–1301. [PubMed: 18451090]
29. Brickman AM, Zahra A, Muraskin J, Steffener J, Holland CM, Habeck C, Borogovac A, Ramos MA, Brown TR, Asllani I, Stern Y. Reduction in cerebral blood flow in areas appearing as white matter hyperintensities on magnetic resonance imaging. Psychiatry Res Neuroimaging. 2009; 172:117–120.
30. Markus HS, Lythgoe DJ, Ostegaard L, O'Sullivan M, Williams SC. Reduced cerebral blood flow in white matter in ischaemic leukoaraiosis demonstrated using quantitative exogenous contrast based perfusion MRI. J Neurol Neurosurg Psychiatry. 2000; 69:48–53. [PubMed: 10864603]
31. Makedonov I, Black SE, MacIntosh BJ. Cerebral small vessel disease in aging and Alzheimer's disease: A comparative study using MRI and SPECT. Eur J Neurol. 2013; 20:243–250. [PubMed: 22742818]
32. Gao FQ, Swartz RH, Scheltens P, Leibovitch FS, Kiss A, Honjo K, Black SE. Complexity of MRI white matter hyperintensity assessments in relation to cognition in aging and dementia from the sunnybrook dementia study. J Alzheimers Dis. 2011; 2:679–688.

33. Leys D, Soetaert G, Petit H, Fauquette A, Pruvo J-P, Steinling M. Periventricular and white matter magnetic resonance imaging hyperintensities do not differ between Alzheimer's disease and normal aging. Arch Neurol. 1990; 47:524–527. [PubMed: 2334300]
34. Pantoni L, Garcia JH. Pathogenesis of leukoaraiosis: A review. Stroke. 1997; 28:652–659. [PubMed: 9056627]
35. Barker R, Ashby EL, Wellington D, Barrow VM, Palmer JC, Kehoe PG, Esiri MM, Love S. Pathophysiology of white matter perfusion in Alzheimer's disease and vascular dementia. Brain. 2014; 137:1524–1532. [PubMed: 24618270]
36. Gouw AA, Seewann A, Vrenken H, van der Flier WM, Rozemuller JM, Barkhof F, Scheltens P, Geurts JJG. Heterogeneity of white matter hyperintensities in Alzheimer's disease: Post-mortem quantitative MRI and neuropathology. Brain. 2008; 131:3286–3298. [PubMed: 18927145]
37. Lo RY, Jagust WJ, Weiner MW, Aisen P. Vascular burden and Alzheimer disease pathologic progression. Neurology. 2012; 79:1349–1355. [PubMed: 22972646]
38. Hirono N, Kitagaki H, Kazui H, Hashimoto M, Mori E. Impact of white matter changes on clinical manifestation of Alzheimer's disease: A quantitative study. Stroke. 2000; 31:2182–2188. [PubMed: 10978049]
39. Jacobs HIL, Clerx L, Gronenschild EHBM, Aalten P, Verhey FRJ. White matter hyperintensities are positively associated with cortical thickness in Alzheimer's disease. J Alzheimers Dis. 2014; 39:409–422. [PubMed: 24169238]
40. Salat DH, Tuch DS, van der Kouwe AJW, Greve DN, Pappu V, Lee SY, Hevelone ND, Zaleta AK, Growdon JH, Corkin S, Fischl B, Rosas HD. White matter pathology isolates the hippocampal formation in Alzheimer's disease. Neurobiol Aging. 2010; 31:244–256. [PubMed: 18455835]
41. Jack CR, Bernstein MA, Fox NC, Thompson P, Alexander G, Harvey D, Borowski B, Britson PJL, Whitwell J, Ward C, Dale AM, Felmlee JP, Gunter JL, Hill DLG, Killiany R, Schuff N, Fox-Bosetti S, Lin C, Studholme C, DeCarli CS, Krueger G, Ward HA, Metzger GJ, Scott KT, Mallozzi R, Blezek D, Levy J, Debbins JP, Fleisher AS, Albert M, Green R, Bartzokis G, Glover G, Mugler J, Weiner MW. The Alzheimer's Disease Neuroimaging Initiative (ADNI): MRI methods. J Magn Reson Imaging. 2008; 27:685–691. [PubMed: 18302232]
42. McKhann G, Drachman D, Folstein M, Katzman R, Price D, Stadlan EM. Clinical diagnosis of Alzheimer's disease: Report of the NINCDS-ADRDA Work Group under the auspices of Department of Health and Human Services Task Force on Alzheimer's Disease. Neurology. 1984; 34:939–944. [PubMed: 6610841]
43. Morris JC. The clinical dementia rating (CDR): Current version and scoring rules. Neurology. 1993; 43:2412–2414.
44. Yendiki A, Koldewyn K, Kakunoori S, Kanwisher N, Fischl B. Spurious group differences due to head motion in a diffusion MRI study. Neuroimage. 2014; 88:79–90. [PubMed: 24269273]
45. Fischl B, Salat DH, Busa E, Albert M, Dieterich M, Haselgrove C, van der Kouwe A, Killiany R, Kennedy D, Klaveness S, Montillo A, Makris N, Rosen B, Dale AM. Whole brain segmentation: Automated labeling of neuroanatomical structures in the human brain. Neuron. 2002; 33:341–355. [PubMed: 11832223]
46. Fischl B, Sereno M, Dale A. Cortical surface-based analysis. I. Segmentation and surface reconstruction. Neuroimage. 1999; 9:179–194. [PubMed: 9931268]
47. Dickerson BC, Bakkour A, Salat DH, Feczko E, Pacheco J, Greve DN, Grodstein F, Wright CI, Blacker D, Rosas HD, Sperling RA, Atri A, Growdon JH, Hyman BT, Morris JC, Fischl B, Buckner RL. The cortical signature of Alzheimer's disease: Regionally specific cortical thinning relates to symptom severity in very mild to mild AD dementia and is detectable in asymptomatic amyloid-positive individuals. Cereb Cortex. 2009; 19:497–510. [PubMed: 18632739]
48. Du AT, Schuff N, Laakso MP, Zhu XP, Jagust WJ, Yaffe K, Kramer JH, Miller BL, Reed BR, Norman D, Chui HC, Weiner MW. Effects of subcortical ischemic vascular dementia and AD on entorhinal cortex and hippocampus. Neurology. 2002; 58:1635–1641. [PubMed: 12058091]
49. Laakso M, Partanen K, Riekkinen P, Lehtovirta M, Helkala EL, Hallikainen M, Hanninen T, Vainio P, Soininen H. Hippocampal volumes in Alzheimer's disease, Parkinson's disease with and without dementia, and in vascular dementia. Neurology. 1996; 46:678–681. [PubMed: 8618666]

50. Greve DN, Fischl B. Accurate and robust brain image alignment using boundary-based registration. Neuroimage. 2009; 48:63–72. [PubMed: 19573611]
51. Smith SM, Jenkinson M, Johansen-Berg H, Rueckert D, Nichols TE, Mackay CE, Watkins KE, Ciccarelli O, Cader MZ, Matthews PM, Behrens TEJ. Tract-based spatial statistics: Voxelwise analysis of multi-subject diffusion data. Neuroimage. 2006; 31:1487–1505. [PubMed: 16624579]
52. Coutu J-P, Chen JJ, Rosas HD, Salat DH. Non-Gaussian water diffusion in aging white matter. Neurobiol Aging. 2014; 35:1412–1421. [PubMed: 24378085]
53. Teipel SJ, Meindl T, Wagner M, Kohl T, Bürger K, Reiser MF, Herpertz S, Möller HJ, Hampel H. White matter microstructure in relation to education in aging and Alzheimer's disease. J Alzheimers Dis. 2009; 17:571–583. [PubMed: 19433891]
54. Leritz EC, Shepel J, Williams VJ, Lipsitz LA, McGlinchey RE, Milberg WP, Salat DH. Associations between T(1) white matter lesion volume and regional white matter microstructure in aging. Hum Brain Mapp. 2014; 35:1085–1100. [PubMed: 23362153]
55. Fazekas F, Kapeller P, Schmidt R, Offenbacher H, Payer F, Fazekas G. The relation of cerebral magnetic resonance signal hyperintensities to Alzheimer's disease. J Neurol Sci. 1996; 142:121–125. [PubMed: 8902731]
56. Brinker T, Stopa E, Morrison J, Klinge P. A new look at cerebrospinal fluid circulation. Fluids Barriers CNS. 2014; 11:10. [PubMed: 24817998]
57. Moftakhar P, Lynch MD, Pomakian JL, Vinters HV. Aquaporin expression in the brains of patients with or without cerebral amyloid angiopathy. J Neuropathol Exp Neurol. 2010; 69:1201–1209. [PubMed: 21107133]
58. Anderson VC, Lenar DP, Quinn JF, Rooney WD. The blood-brain barrier and microvascular water exchange in Alzheimer's disease. Cardiovasc Psychiatry Neurol. 2011; 2011:615829. [PubMed: 21687589]
59. Taheri S, Gasparovic C, Huisa BN, Adair JC, Edmonds E, Prestopnik J, Grossetete M, Shah NJ, Wills J, Qualls C, Rosenberg GA. Blood-brain barrier permeability abnormalities in vascular cognitive impairment. Stroke. 2011; 42:2158–2163. [PubMed: 21719768]
60. Zlokovic BV. Neurovascular pathways to neurodegeneration in Alzheimer's disease and other disorders. Nat Rev Neurosci. 2011; 12:723–738. [PubMed: 22048062]

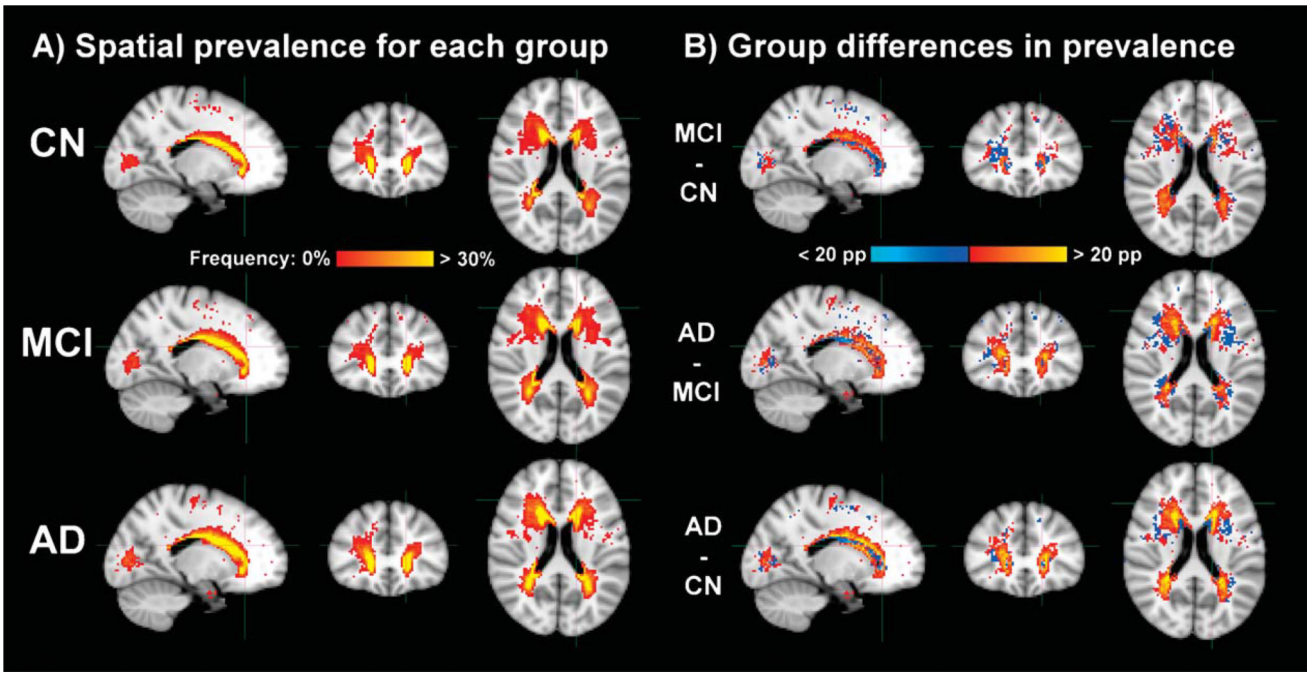

Fig. 1.

A) Spatial prevalence of WMC in controls (CN) and individuals with mild cognitive impairment (MCI) and Alzheimer's disease (AD). Color scale varies from red to yellow, from when at least one participant has WMC to when 30% or more have WMC in a given voxel. The cap of 30% allows easier comparison of the diffuse differences between groups. B) Group differences in spatial prevalence of WMC. Color scale varies from light blue to blue for negative differences of −20 to −1 percentage points and from red to yellow for positive differences of 1 to 20 percentage points. All results are displayed in the common MNI152 space after using FSL FNIRT for proper nonlinear registration of the subcortical structures.

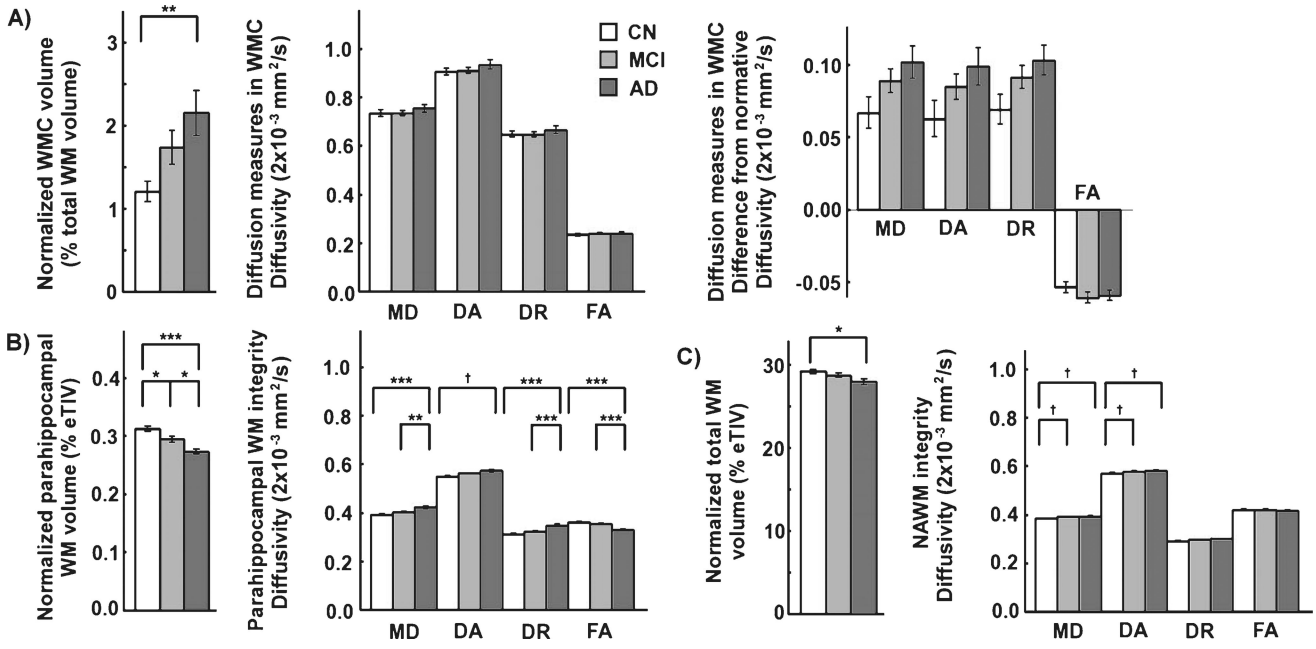

Fig. 2.

Group comparisons of volume and diffusion measures of a) WMC, b) parahippocampal WM and c) NAWM. The volume of WMC is normalized to the total WM volume. Parahippocampal and total WM volumes are normalized by the eTIV. Group differences were statistically assessed with the post-hoc Tukey test for each volume and diffusion measure, correcting for age, gender, education and motion measures (*, ** and *** for corrected $p < 0.05$, 0.01 and 0.001 respectively, † for uncorrected $p < 0.05$). The difference between diffusion properties of WMC and the corresponding diffusion properties in a non-lesioned normative brain is shown in addition to the absolute diffusion properties of WMC. The analyses involving diffusion measures in WMC were limited to individuals with a volume of WMC greater than 1% total WM volume. The log-transform of the normalized volume of WMC was used for statistical purposes. Standard error bars are shown. (MD, DA, and DR, mean, axial and radial diffusivity; FA, fractional anisotropy; WMC, white matter changes; WM, white matter; NAWM, normal-appearing white matter; eTIV, estimated total intracranial volume; CN, control; MCI, mild cognitive impairment; AD, Alzheimer's disease).

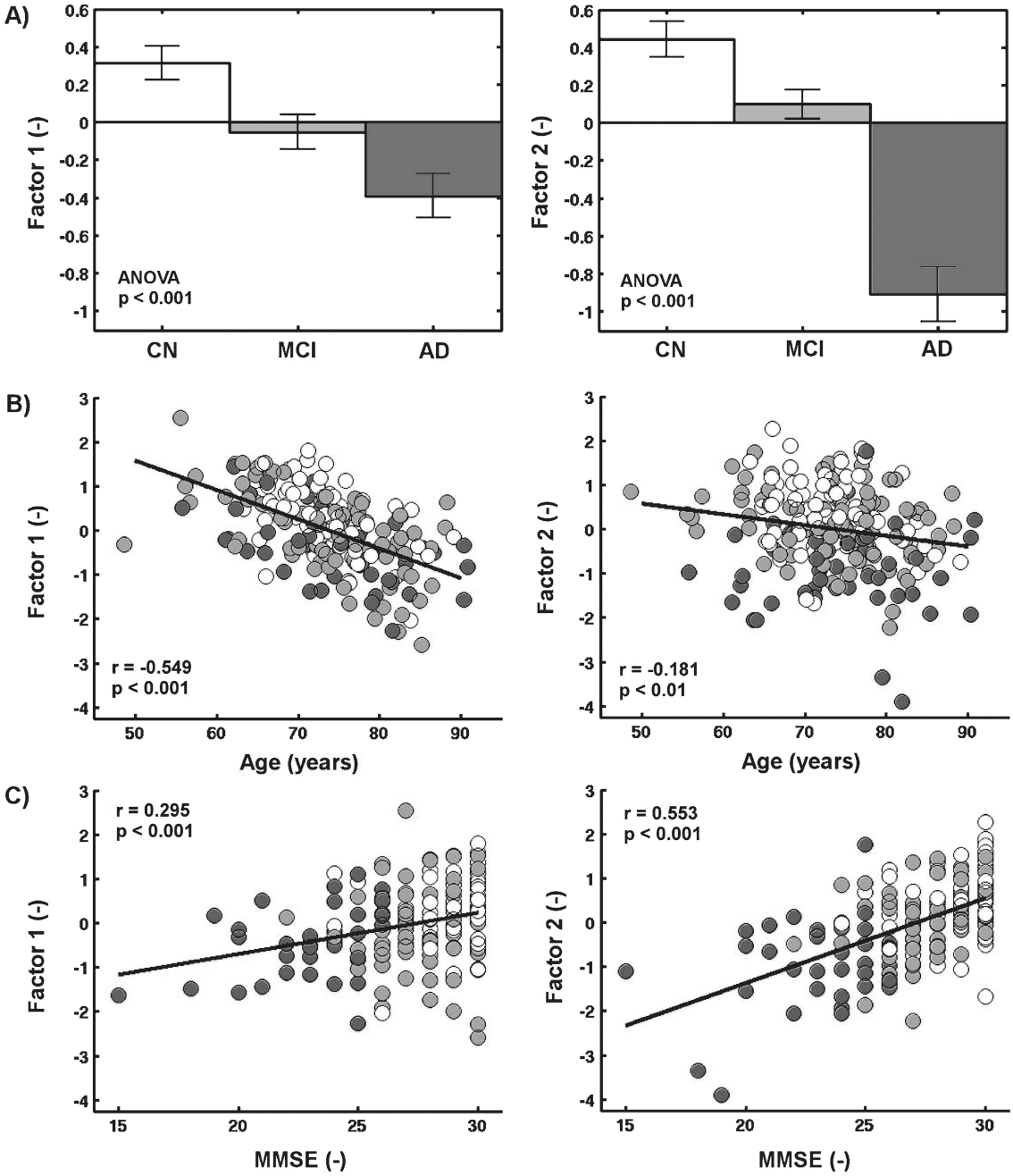

Fig. 3.

Factor scores in relation to a) group, b) age and c) Mini-Mental State Examination (MMSE). Controls (CN), individuals with mild cognitive impairment (MCI) and Alzheimer's disease (AD) are shown respectively in white, light gray, and dark gray. The presence of group differences was statistically confirmed using ANOVA and the Steiger z test confirmed that Factor 1 had a stronger age effect ($p < 0.001$) and a weaker MMSE effect ($p < 0.01$) than Factor 2. Standard error bars are shown.

Table 1

Demographics for all participants

	CN	MCI	AD	*p*-value
All ADNI, *n* = 215				
Participants (female)	73 (46)	96 (36)	46 (17)	**0.0016**
Age (years)	72.98 (0.84)	73.80 (0.73)	74.58 (1.06)	0.4900
Education (years)	16.30 (0.32)	16.10 (0.28)	15.24 (0.41)	0.1086
MMSE (−)[a]	28.67 (0.25)	27.88 (0.22)	23.14 (0.32)	**<0.0001**
APOE ε4 (# alleles)[b]	0.32 (0.10)	0.64 (0.07)	0.88 (0.11)	**0.0006**
Translation motion (mm)	1.32 (0.07)	1.34 (0.06)	1.35 (0.09)	0.9671
Rotation motion (degrees)	0.0062 (0.0003)	0.0063 (0.0003)	0.0068 (0.0004)	0.5621
Volume of WMC[*] (cc)	4.93 (0.75)	7.10 (0.66)	8.85 (0.95)	**0.0046**
Total WM volume (cc)	415.71 (6.46)	426.08 (5.63)	408.59 (8.13)	0.1783
Ventricular volume (cc)	30.56 (1.96)	36.59 (1.71)	44.46 (2.46)	**<0.0001**
Hippocampal volume (cc)	7.64 (0.12)	6.81 (0.10)	5.79 (0.15)	**<0.0001**
ADNI subgroup with WMC volume >1% total WM volume, *n* = 118				
Participants (female)	30 (17)	54 (20)	34 (9)	**0.0436**
Age (years)	75.74 (1.24)	76.61 (0.93)	77.05 (1.17)	0.7356
Education (years)	16.30 (0.54)	16.22 (0.40)	15.41 (0.51)	0.3774
MMSE (−)[c]	28.17 (0.49)	27.64 (0.30)	22.48 (0.41)	**<0.0001**
APOE ε4 (# alleles)[d]	0.18 (0.16)	0.65 (0.09)	0.78 (0.12)	**0.0108**
Translation motion (mm)	1.35 (0.11)	1.46 (0.08)	1.48 (0.11)	0.6372
Rotation motion (degrees)	0.0063 (0.0005)	0.0069 (0.0004)	0.0073 (0.0005)	0.4292
Volume of WMC[*] (cc)	8.33 (1.31)	10.68 (0.98)	11.06 (1.23)	0.2556
Total WM volume (cc)	414.12 (11.08)	425.13 (8.26)	411.60 (10.41)	0.5395
Ventricular volume (cc)	36.33 (3.23)	43.03 (2.41)	48.90 (3.04)	**0.0208**
Hippocampal volume (cc)	7.39 (0.18)	6.49 (0.13)	5.69 (0.17)	**<0.0001**

All significant *p*-values are bolded. Standard errors are shown in parentheses. (MMSE, Mini-Mental State Exam; CN, control; MCI, mild cognitive impairment; AD, Alzheimer's disease; WM, white matter; WMC, white matter changes).

[a] Information missing for 16 CN, 20 MCI and 11 AD.

[b] Information missing for 29 CN, 5MCI and 12 AD.

[c] Information missing for 12 CN, 7MCI and 9 AD.

[d] Information missing for 13 CN, 3 MCI and 7 AD.

[*] Caution should be exercised when comparing with volumes of white matter hyperintensities obtained with T_2-weighted and FLAIR MRI which are very strongly correlated with WMC volumes obtained with FreeSurfer but approximately 1.14 times greater than WMC volumes.

Table 2

Models of the diffusion parameters in WMC, parahippocampal and normal-appearing WM with all neuroimaging markers

Parameters	MD (β; *p*-value)	DA (β; *p*-value)	DR (β; *p*-value)	FA (β; *p*-value)
Model 1	WMC (subgroup with volume >1% total WM volume, *n* = 118)			
Group (MCI)	0.03; 0.6332	0.04; 0.5480	0.02; 0.6976	0.01; 0.8862
Group (AD)	0.11; 0.1604	0.07; 0.3995	0.14; 0.0912	*−0.27; 0.0229*
Age	0.07; 0.1938	0.04; 0.4654	0.08; 0.1118	*−0.18; 0.0167*
Gender (female)	0.04; 0.4210	0.03; 0.4923	0.04; 0.3949	−0.06; 0.3937
Education	*0.10; 0.0280*	0.08; 0.0631	*0.11; 0.0200*	−0.12; 0.0831
Cortical thickness	0.03; 0.6039	−0.01; 0.8331	0.05; 0.3521	***−0.24; 0.0029**
Hippocampal vol.	0.08; 0.2628	0.07; 0.3264	0.08; 0.2439	−0.13; 0.2131
Ventricular volume	****0.55; <0.0001**	****0.60; <0.0001**	****0.51; <0.0001**	0.15; 0.0712
Volume of WMC	***−0.26; 0.0015**	****−0.27; 0.0007**	***−0.25; 0.0026**	−0.07; 0.4984
Total WM volume	*−0.15; 0.0042*	*−0.14; 0.0085*	***−0.16; 0.0036**	0.12; 0.1270
Norm. properties	****0.55; <0.0001**	****0.50; <0.0001**	****0.57; <0.0001**	****0.61; <0.0001**
Translation motion	*0.21; 0.0218*	0.13; 0.1435	*0.26; 0.0069*	****−0.50; 0.0002**
Rotation motion	*−0.19; 0.0350*	−0.14; 0.1144	*−0.22; 0.0187*	*0.29; 0.0254*
Model 2	Parahippocampal WM (all, *n* = 215)			
Group (MCI)	−0.08; 0.3057	−0.02; 0.8662	−0.11; 0.1425	0.13; 0.0802
Group (AD)	0.16; 0.1809	0.06; 0.6554	0.20; 0.0756	*−0.23; 0.0367*
Age	0.03; 0.6548	−0.00; 0.9909	0.05; 0.4887	−0.11; 0.1210
Gender (female)	−0.01; 0.8554	−0.06; 0.4412	0.01; 0.8476	−0.11; 0.0633
Education	0.05; 0.4451	0.01; 0.8321	0.06; 0.2978	−0.10; 0.0900
Cortical thickness	−0.11; 0.1440	−0.02; 0.7771	*−0.15; 0.0391*	*0.19; 0.0091*
Hippocampal vol.	****−0.32; 0.0008**	***−0.31; 0.0038**	****−0.30; 0.0007**	*0.19; 0.0274*
Ventricular volume	0.02; 0.8150	0.00; 0.9282	0.03; 0.7291	0.01; 0.9291
Volume of WMC	0.13; 0.1038	0.15; 0.1004	0.11; 0.1361	−0.05; 0.5017
Total WM volume	−0.02; 0.8370	0.11; 0.2064	−0.08; 0.2762	***0.23; 0.0012**
Translation motion	−0.01; 0.9051	0.03; 0.8128	−0.03; 0.7428	0.08; 0.4395
Rotation motion	0.11; 0.3269	0.01; 0.9165	0.16; 0.1505	*−0.25; 0.0216*
Model 3	Normal-appearing white matter (all, *n* = 215)			
Group (MCI)	0.11; 0.0994	*0.17; 0.0323*	0.09; 0.2027	0.02; 0.8058
Group (AD)	−0.09; 0.3685	−0.10; 0.4079	−0.09; 0.3804	0.07; 0.5049
Age	0.09; 0.1603	0.13; 0.0694	0.07; 0.2754	0.00; 0.9891
Gender (female)	0.05; 0.3410	0.06; 0.3216	0.05; 0.3855	−0.04; 0.5233
Education	0.10; 0.0574	0.10; 0.1040	0.10; 0.0550	−0.07; 0.2079
Cortical thickness	−0.08; 0.2342	−0.07; 0.3574	−0.08; 0.2104	0.03; 0.6393

Parameters	MD (β; *p*-value)	DA (β; *p*-value)	DR (β; *p*-value)	FA (β; *p*-value)
Hippocampal vol.	−0.05; 0.5035	−0.16; 0.0741	−0.00; 0.9772	−0.09; 0.2914
Ventricular volume	0.04; 0.5349	0.11; 0.1534	0.01; 0.8824	0.11; 0.1174
Volume of WMC	***0.36; <0.0001	*0.20; 0.0108*	***0.42; <0.0001	***−0.51; <0.0001
Total WM volume	*−0.14; 0.0323*	−0.02; 0.7400	*−0.19; 0.0033	**0.23; 0.0005
Translation motion	−0.15; 0.1322	*−0.29; 0.0100*	−0.08; 0.4058	−0.16; 0.1094
Rotation motion	***0.40; <0.0001	***0.48; <0.0001	**0.36; 0.0003	−0.16; 0.1068

All continuous variables were standardized prior to applying the model for easier comparison of parameter estimates (β).

Uncorrected *p*-values are presented and significant associations with corrected $p < 0.05$ are bolded (*, ** and *** for corrected $p < 0.05$, 0.01 and 0.001 respectively).

Associations with uncorrected $p < 0.05$ are italicized. (WMC, white matter changes; WM, white matter).

Table 3

Factor analysis of highly correlated neuroimaging markers in Alzheimer's disease

Parameters	Factor 1	Factor 2
Volume of WMC	**−0.642**	−0.270
Total WM volume	**0.694**	0.052
Ventricular volume	**−0.685**	−0.288
Hippocampal volume	**0.630**	**0.405**
Cortical thickness	0.225	**0.946**

Coefficients higher than 0.40 are bolded to indicate the most important markers contributing to each significant factor. (WMC, white matter changes; WM, white matter).

Table 4

Models of the diffusion parameters in WMC, parahippocampal and normal-appearing WM with factors extracted from the neuroimaging markers

Parameters	MD (β; *p*-value)	DA (β; *p*-value)	DR (β; *p*-value)	FA (β; *p*-value)
Model 4	WMC (subgroup with volume >1% total WM volume, *n* = 118)			
Group (MCI)	0.01; 0.8798	0.02; 0.7787	0.00; 0.9526	0.02; 0.8207
Group (AD)	−0.05; 0.6085	−0.10; 0.2634	−0.01; 0.9043	*−0.25; 0.0296*
Age	−0.00; 0.9990	−0.02; 0.7591	0.01; 0.8300	***−0.22; 0.0032**
Gender (female)	0.05; 0.3867	0.05; 0.3649	0.05; 0.3834	−0.12; 0.0967
Education	*0.13; 0.0202*	*0.11; 0.0499*	*0.14; 0.0129*	−0.11; 0.1103
Factor 1	****−0.50; <0.0001**	****−0.52; <0.0001**	****−0.47; <0.0001**	−0.10; 0.2073
Factor 2	*−0.17; 0.0050*	***−0.23; 0.0003**	*−0.14; 0.0262*	****−0.32; <0.0001*
Norm. properties	****0.88; <0.0001**	****0.85; <0.0001**	****0.88; <0.0001**	****0.57; <0.0001**
Translation motion	0.06; 0.5509	−0.02; 0.8665	0.11; 0.2917	***−0.49; 0.0003**
Rotation motion	−0.12; 0.2770	−0.06; 0.5828	−0.15; 0.1672	*0.29; 0.0360*
Model 5	Parahippocampal WM (all, *n* = 215)			
Group (MCI)	−0.06; 0.4451	0.01; 0.9214	−0.09; 0.2168	0.12; 0.0989
Group (AD)	*0.24; 0.0390*	0.14; 0.2821	*0.28; 0.0121*	*−0.28; 0.0098*
Age	0.06; 0.3914	0.03; 0.7563	0.08; 0.2599	*−0.14; 0.0416*
Gender (female)	−0.05; 0.4092	−0.11; 0.1036	−0.02; 0.7927	*−0.12; 0.0294*
Education	0.04; 0.5012	0.01; 0.9297	0.06; 0.3269	−0.10; 0.0909
Factor 1	****−0.32; <0.0001**	*−0.19; 0.0317*	****−0.36; <0.0001**	****0.35; <0.0001*
Factor 2	***−0.22; 0.0019**	−0.13; 0.0991	***−0.25; 0.0002**	***0.24; 0.0003**
Translation motion	0.04; 0.7069	0.10; 0.4426	0.01;0.9173	0.07; 0.5302
Rotation motion	0.07; 0.5298	−0.04; 0.7845	0.12; 0.2564	*−0.24; 0.0274*
Model 6	Normal-appearing white matter (all, *n* = 215)			
Group (MCI)	0.12; 0.0935	*0.17; 0.0243*	0.09; 0.2087	0.01; 0.8535
Group (AD)	−0.14; 0.1812	−0.09; 0.4349	−0.15; 0.1297	0.16; 0.1469
Age	*0.13; 0.0381*	*0.14; 0.0409*	0.12; 0.0534	−0.08; 0.2365
Gender (female)	0.06; 0.2490	0.04; 0.5131	0.07; 0.1881	−0.08; 0.1667
Education	0.08; 0.1431	0.09; 0.1312	0.07; 0.1834	−0.03; 0.6176
Factor 1	****−0.44; <0.0001**	***−0.35; 0.0003**	****−0.46; <0.0001**	****0.39; <0.0001**
Factor 2	***−0.19; 0.0023**	*−0.18; 0.0066*	***−0.18; 0.0029**	0.10; 0.1356
Translation motion	−0.13; 0.1977	*−0.27; 0.0166*	−0.06; 0.5319	−0.19; 0.0917
Rotation motion	***0.40; 0.0001**	****0.46; <0.0001**	***0.35; 0.0006**	−0.16; 0.1407

All continuous variables were standardized prior to applying the model for easier comparison of parameter estimates (β).

Uncorrected *p*-values are presented and significant associations with corrected $p < 0.05$ are bolded (*, ** and *** for corrected $p < 0.05$, 0.01 and 0.001 respectively).

Associations with uncorrected $p < 0.05$ are italicized. (WMC, white matter changes; WM, white matter).